GRAPHICAL ABSTRACT

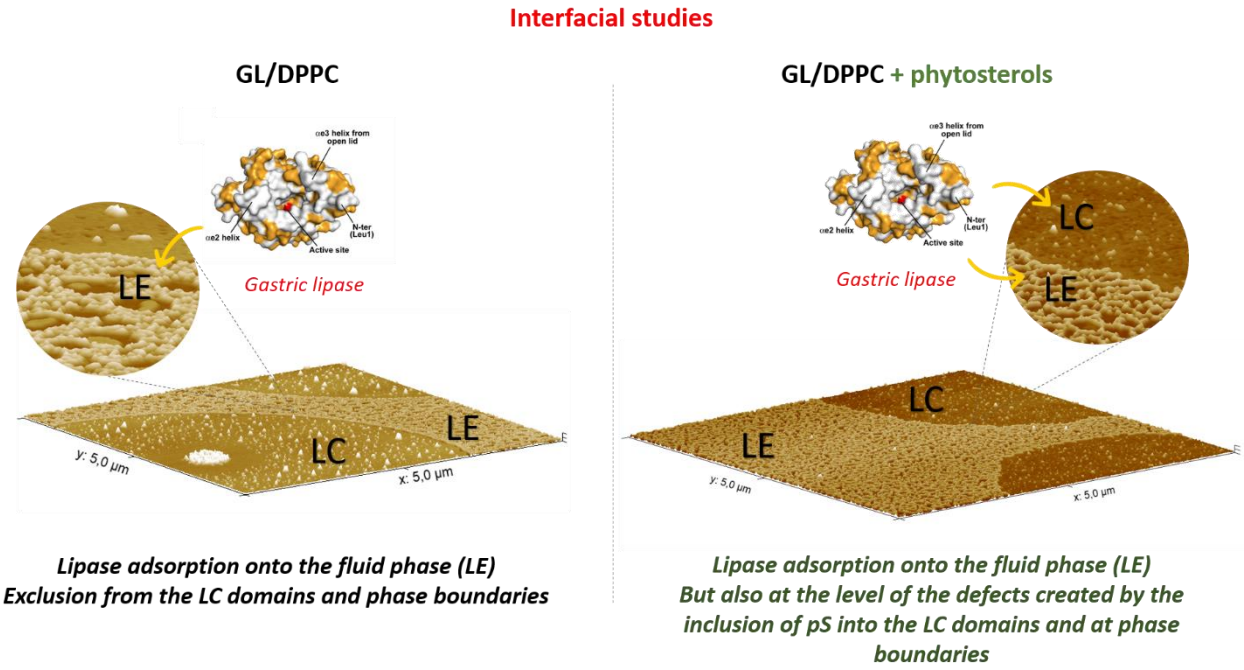

HIGHLIGHTS

- rDGL binds to the fluid phase of homogeneous galactolipid monolayer.
- The orientation of galactolipid polar heads limits the adsorption capacity of rDGL.
- rDGL was excluded from condensed phase domains in mixed heterogenous galactolipid-phospholipid monolayer.
- Defects created in the condensed phase by addition of phytosterol favor rDGL adsorption.

Title: Modulation of gastric lipase adsorption onto mixed galactolipid-phospholipid films by addition of phytosterols

Name(s) of Author(s) Jeanne Kergomard[1,2], Frédéric Carrière[3], Gilles Paboeuf[1], Nathalie Barouh[4,5], Claire Bourlieu-Lacanal[2] & Véronique Vié[1,6]*

Author Affiliation(s) [1] IPR Institute of Physics, UMR UR1 CNRS 6251, Rennes 1 University, France; [2]INRAE/UM/Institut Agro Montpellier UMR 1208 IATE, France; [3]Aix-Marseille Université, CNRS, UMR7281 Bioénergétique et Ingénierie des Protéines, Marseille, France ; [4]CIRAD, UMR QUALISUD, F34398 Montpellier-France, [5]Qualisud, Univ Montpellier, Avignon Université, CIRAD, Institut Agro, Université de La Réunion, Montpellier, France, [6]Univ Rennes 1, CNRS, ScanMAT - UMS 2001, F-35042 Rennes, France.

*C**orresponding author: Dr. Véronique Vié, Institut de Physique de Rennes, Campus de Beaulieu, UMR UR1 CNRS 6251, Université de Rennes 1, 35042 Rennes cedex,** phone number: 33 (0)2 23 23 56 45 and E-mail address : veronique.vie@univ-rennes1.fr; **Dr. C. Bourlieu-Lacanal, UMR 1208 IATE, 2 Place Pierre Viala, Bât. 31, INRAE/UM/Institut Agro Montpellier, F34060 MONTPELLIER CEDEX 1**, France, phone number: 33 (0)4 99 61 22 03 and E-mail address : claire.bourlieu-lacanal@inrae.fr

Present/permanent address: Institut de Physique de Rennes, campus de Beaulieu, 35042 Rennes cedex – France

Word count: 6527

Total number of tables/figures: 7

Abbreviations

AFM: atomic force microscopy

BMM: bovine milk membranes

DGDG: digalactosyldiacylglycerol

DPPC: dipalmitoylphosphatidylcholine

GL: galactolipids

HGL: human gastric lipase

HMM: human milk membranes

IRS: Interfacial recognition site

LC: liquid condensed phase

LE: liquid expanded phase

MGDG: monogalactosyldiacylglycerol

MPL: milk polar lipids

PTL: pancreatic triacylglycerol lipase

rDGL: recombinant dog gastric lipase

ABSTRACT

The rapid and preferential adsorption of a gastric lipase recombinant dog gastric lipase (rDGL) in heterogeneous films of phospholipids and triacylglycerols has previously been unveiled using Langmuir films analyzed by tensiometry, ellipsometry and Langmuir-Blodgett transfer coupled to atomic force microscopy. Here we invest the adsorption behavior of rDGL in heterogeneous galactolipid and mixed galactolipid-phospholipid or galactolipid-phospholipid-phytosterol films representative of plant membrane. Again rDGL, preferentially got adsorbed at the expanded lipid phases of the films underlining the genericity of such adsorption behavior. The addition of phytosterols to these mixtures resulted in the creation of defects, favoring the adsorption of rDGL at the fluid phases, but also improving the adsorption capacities of the lipase at the phase boundaries and towards the defects in the condensed phase. rDGL, like all gastric lipases, does not show any activity on galactolipids and phospholipids but its adsorption impacts their lateral organization and may change the adsorption and activity of other lipolytic enzymes in the course of digestion.

KEYWORDS: adsorption, gastric lipase, galactolipids, heterogeneous biomimetic membranes, plant lipids, ellipsometry/tensiometry, atomic force microscopy

1 INTRODUCTION

Lipases (EC 3.1.1.3, triacylglycerol hydrolase) play an important role in lipid metabolism, and have been found in most living organisms, from the plant kingdom to microorganisms and animals (Huang, 1987; Jaeger et al., 1994). Lipases are water-soluble enzymes that catalyze the hydrolysis of the ester bonds of insoluble triacylglycerols (TAG). Prior to the hydrolysis of their substrates, lipases must therefore get adsorbed onto the lipid-water interface (Aloulou et al., 2006). The digestion of lipids is a complex phenomenon, which depends on their chemical structure, their organization in water (monolayers, bilayers, micelles, oil/water emulsions…) and the ability of lipolytic enzymes to interact with these lipid assemblies. Indeed, the mechanisms involved in enzymatic lipolysis depends on the interfacial organization of the lipid substrates.

In humans, lipid digestion starts in the stomach where gastric lipase is responsible for 10% to 25% of the TAG total digestion (Carrière et al., 2001; Lengsfeld et al., 2004) and is very central during neonatal period as it is mature at birth (Bourlieu et al., 2015). It is worth nothing that gastric lipase is a true lipase, acting on TAG digestion but not on polar lipids, such as phospholipids or galactolipids. Human gastric lipase (HGL) is a globular enzyme of 50 kDa, belonging to the α/β hydrolase family, and possessing a classical Ser-His-Asp catalytic triad (Canaan et al., 1999; Roussel et al., 1999). The active site is covered by a lid, which has to be displaced to permit the TAG substrates to have access to the enzyme active site. Changes in the conformation (opening) of the lid have been observed in the homologous dog gastric lipase, co-crystallized in the presence of substrate analogs (Roussel et al., 2002). The lid opening generates a large hydrophobic ring, that is part of the interfacial recognition site (IRS) located around the active site entrance (Figure 1).

Gastric lipase has been found to be highly active in the acidic environment of the stomach with an optimum at pH 4-5.4, thanks to a remarkable stability and adsorption capacity at the

lipid/water interface at low pH, in contrast to other lipases (Bénarouche et al., 2013; Chahinian et al., 2006). This pH-dependent interfacial adsorption is driven by hydrophobic interactions between the substrates and the large hydrophobic ring, part of the IRS (Figure 1.B) (Chahinian et al., 2006) and electrostatic interactions, rDGL surface potential being mostly positive at low pH (Figure 1.C). This combination of interactions probably explains why rDGL is a highly tensioactive lipase with a high penetration capacity into phospholipid layers (Bénarouche et al., 2013).

Prior to hydrolyzing TAG, lipases frequently have to get adsorbed onto interfacial films composed of polar lipids and/or amphiphilic proteins (Bénarouche et al., 2017), in which a small fraction of TAG playing various metabolic part can also be found (Lerique et al., 1994). This is typically the case of milk fat globules and phospholipid-stabilized emulsions. Polar lipids are not hydrolyzed in the upper gastrointestinal tract by gastric lipase, but this enzyme has a strong ability to get inserted into phospholipid (PL) monolayers thanks to its high surfactant capacity (Bénarouche et al., 2013; de La Fournière et al., 1994) and thus, has access to the TAG substrate. In addition, gastric lipolysis favors the activity of pancreatic lipase (Gargouri et al., 1986) and has been recently reported to significantly affect the production and the degradation of intermediate TAG digestion products during the intestinal phase (Infantes-Garcia et al., 2021). Given the synergy between the gastric and intestinal digestion phases, it is crucial to obtain knowledge on the protein-lipid interactions occurring during the gastric phase, including the impact of gastric lipase adsorption onto the interfacial organization of membrane lipids, even though gastric lipase is not active on phospholipids (Carrière et al., 1991) nor on galactolipids (Wattanakul et al., 2019).

Polar lipid films are useful tools to study the interfacial properties of lipases, irrespective of their lipolytic activity. Langmuir films used as model interfaces allows determining the impact of various physicochemical parameters, including the lipid packing and composition at the

111 air/water interface, on the adsorption and insertion capacity of a lipase. The variations of surface
112 pressure are related to interactions between molecules, which are directly connected to the
113 variations of molecular areas. The coupling of surface pressure measurements and ellipsometry
114 provides insights on the thickness and refractive index of the surface layer formed, and thus on the
115 phenomena occurring in one micrometer range below the interface.

116 Previous studies have been done on the adsorption behavior of gastric lipase onto model
117 heterogenous films mimicking the outer layer of the membrane of human and bovine milk fat
118 globule (Bourlieu et al., 2016, 2020). These studies have shown that the coexistence of expanded
119 and condensed phases influenced sternly lipase adsorption: lipase got rapidly inserted onto the fluid
120 phase and at the phase boundaries. In addition, different levels of insertion were observed
121 suggesting a molecular cooperation and besides hydrophobic interactions local negative charges
122 reinforced adsorption.

123 However, to the best of our knowledge, no study has yet tackled the question of adsorption
124 and penetration mechanisms of gastric lipase onto plant cell membranes, especially the nature
125 widespread photosynthetic membranes. On the contrary to animal cell membranes, plant
126 photosynthetic membranes to save up phosphorus do not contain phospholipids but
127 galactoglycerophospholipids (or galactolipids), which accounts for more than 70% of polar lipids
128 (Dörmann & Benning, 2002). In addition to their biological and structural functions in membranes,
129 galactolipids are of nutritional importance since they are rich in polyunsaturated fatty acids
130 (PUFA), essentials to cell functions in the human body, and especially in the α-linolenic acid
131 (C18:3 n-3, ALA) (Sahaka et al., 2020). Phytosterols and carotenes are also major constituents of
132 plant cell membranes (Grosjean et al., 2015; Silvius, 2005). They play a key role in maintaining
133 biologic properties of membranes by controlling their structural properties such as their

permeability, fluidity and rigidity (Dufourc, 2008; Silva et al., 2007). The chemical structures of phytosterols are similar to those of animal cholesterol, nevertheless the absorption of the majority of phytosterols in the intestinal tract of mammals is up to ten times lower than that of cholesterol (von Bergmann et al., 2005). In humans, phytosterol consumption has been shown to induce a lowering of plasma cholesterol levels, thus preventing cardiovascular diseases and atherosclerosis (Moghadasian & Frohlich, 1999). Sterol molecules are known to promote hydrophobic interactions between membrane lipid acyl chains, which introduce a higher order and a subsequent rigidification of membranes (Silva et al., 2011). At the air/water interface, the incorporation of phytosterols molecules in a phospholipid film has been shown to reorganize the monolayer, by modifying the packing and orientation of the polar heads of phospholipids (Hąc-Wydro et al., 2007).

In this context, the present work aimed at determining the interaction of gastric lipase with mixed films of galactolipids, galactolipids/phospholipids, and galactolipids/phospholipids/phytosterols, mimicking plant photosynthetic membranes. Biophysical tools such as the combination of ellipsometry and tensiometry were used to monitored the lipid-protein interactions at the air/water interface. Atomic force microscopy was further used to study the distribution of the enzyme into the heterogeneous lipid systems. Recombinant dog gastric lipase (Figure 1) was used as a representative gastric lipase available in a purified and well characterized form (Roussel et al., 1999) and with close homology with human gastric lipase. Vegetal membrane composition was approached using mixed monolayers of purified phospholipids (PL), galactolipids (GL) and phytosterols (pS) presenting liquid expended/liquid condensed (LE/LC) phase coexistence at 20 mN/m and 20°C.

2 EXPERIMENTAL SECTION

Chloroform and methanol were purchased from Sigma Aldrich Ltd. (St. Quentin Fallavier, France). If not stated otherwise, all biophysical characterizations were conducted at least in triplicate.

2.1 Preparation of lipid mixtures

Glycerophospholipids (dipalmitoylphosphatidylcholine, DPPC) and galactolipids (monogalactosyldiacylglycerol, MGDG, and digalactosyldiacylglycerol, DGDG) were purchased from Avanti Polar Lipids (see supplementary data for their fatty acid composition). Canola phytosterols (pS) from the deodorization distillates of canola oil were obtained as a gift from Cognis France (Estarac, France). The typical molar composition (estimated from usual normalized GC procedures) was: β-sitosterol (50.3 mol%), campesterol (38.9 mol%) and brassicasterol (10.5 mol%). β-sitosterol and campesterol are the most commonly found in the human diet due to their high composition in nuts and oilseed species (Cañabate-Díaz et al., 2007; Phillips et al., 2005). Brassicasterol is a phytosterol found in some unicellular algae and terrestrial plants such as rapeseed (Ikekawa et al., 1968; Itoh et al., 1973) .

Simple binary mixture of MGDG and DGDG (60:40, mol/mol) was prepared, namely GL. Ternary and quaternary mixtures of GL, DPPC and pS, namely GL/DPPC (50:50, mol/mol) and GL/DPPC/pS (45:45:10 mol/mol/mol), respectively, were also prepared to mimic the composition of natural vegetal membrane (see Table 1 for relative molar composition). Lipid-lipid interactions and molecular organization at the air/water interface of the three monolayers studied are reported in Kergomard et al. (2022).

2.2 Enzyme purifications and preparation of aliquots

Recombinant dog gastric lipase (rDGL) (86% amino acid sequence identity with HGL) was produced in transgenic maize by Meristem Therapeutics (Clermont-Ferrand, France) and purified as described previously (Roussel et al., 1999). rDGL stock solution was prepared at a concentration of 1.8 mg/mL in 10 mM sodium acetate buffer, 100 mM NaCl, 20 mM $CaCl_2$, pH 5, and stored at -20°C. Diluted aliquots at a final concentration of 1.92 mg/mL (40 nM) were prepared in the same buffer before being used in monolayer experiments.

2.3 Ellipsometry and surface pressure measurements at the air/water interface

Kinetic measurements over 5 hours were performed using circular Teflon trough of 8 mL (surface area of 27 cm^2). Kinetic measurements over 2 hours before Langmuir Blodgett transfer of the interfacial film were performed using Langmuir trough of 50 mL and a surface area of 35 cm^2.

Before each experiment, the Teflon trough have been carefully cleaned with UP water and ethanol to get rid of surface-active residual impurities. Control ellipsometric and tensiometric measurements were performed during half an hour on 10 mM acetate buffer, 100 mM NaCl, 20 mM $CaCl_2$, pH 5 before experiments to check the cleaned surface before experiments. The surface pressure (π) and the ellipsometric angle (Δ) were recorded at the same time. π was measured according to the Wilhelmy-plate method using a filter paper connected to a microelectronic feedback system to measure the surface pressure (Nima Technology, UK). Values of π were recorded every 4 s with a precision of ± 0.2 mN/m. Ellipsometric measurements were carried out using a home-made automated ellipsometer in a "null ellipsometer" configuration (Berge & Renault, 1993; Bourlieu et al., 2020). The laser beam probed a surface of 1 mm^2 and a depth in the

order of 1 µm and provided insight on the thickness of the interfacial film formed at the interface. Values of the ellipsometric angle (Δ, °) were recorded every 4 s with a precision of ± 0.5 °.

2.4 Adsorption of rDGL onto multicomponent lipid monolayers and at the air/water interface

A homogenous monolayer was formed by spreading a few microliters of 1 mM solution of lipids in $CHCl_3$/MeOH (2:1, v/v) over the surface of the buffer solution until an initial pressure of 20 ± 1 mN/m was reached (Bénarouche et al., 2013). After stabilization of the film over 5 minutes, rDGL was further injected in the sub-phase at a final concentration of 40 nM. The increase of the surface pressure and ellipsometric angle due to protein adsorption onto the lipid monolayer was continuously monitored until reaching the equilibrium.

2.5 Visualization of phase separations and lipase distribution in heterogeneous film by atomic force microscopy

For AFM imaging, interfacial films were transferred onto a freshly-cleaved mica plate using the Langmuir-Blodgett method. The transfer was processed after 2 hours kinetics at a constant surface pressure and at a very low speed (0.5 $mm.min^{-1}$). Imaging was carried out with an AFM (Multimode Nanoscope 5, Bruker, France) in contact mode QNM in air (20°C), using a standard silicon cantilever (0.06 N/m, SNL-10, Bruker, France), and at a scan rate of 1 Hz. The force was minimized during all scans and the scanner size was 100×100 $µm^2$. The processed images analyzed by the open-source platform Gwyddion are representative of at least duplicated experiments. ImageJ software was used to perform the analysis of AFM images. The functions *Plot Profile*, *Threshold*, *Particle Analysis*, *Make Binary* and *Dilate* were applied to study the different height levels as well as the shape of the protein networks. ImageJ software was used to perform different height analyses

(based on the analyses of five plot profiles taken randomly in the AFM image) and thresholds on the raw AFM images (see supplementary data), in line with the study of Bourlieu et al. (2016)

3 RESULTS

3.1. Ellipsometric and tensiometric adsorption kinetics of rDGL onto galactolipids (homogenous phase) and mixed galactolipid-phospholipids (heterogenous phase) monolayers

The adsorption kinetics of rDGL onto the GL monolayer was studied by tensiometry and ellipsometry, at 20 mN/m. Under these conditions, the GL monolayer forms a liquid expanded (LE) phase. The results obtained on this homogenous system were then compared with the rDGL adsorption kinetics onto heterogenous film based on mixture of galactolipids and phospholipids (GL/DPPC monolayer). Under these conditions, some phase separation occurs with the coexistence of liquid condensed (LC) and LE phases at 20 mN/m.

The gastric lipase was injected into the subphase after 5 minutes equilibrium of the GL and GL/DPPC lipid films, respectively. The adsorption kinetics were monitored over five hours. The variations with time in the ellipsometric angle and surface pressure are shown Figure 2.

In Figure 2.A, the surface pressure increased quickly after the injection of the enzyme in the subphase below the GL monolayer, while the ellipsometric angle remained stable over the first few minutes of kinetics, reflecting the accumulation of the gastric lipase below the air/water interface. After one hour kinetic, the surface pressure started to slowly decrease, together with a drastic increase in the ellipsometric angle from 6.9° to a maximum value of 12.9°, reflecting a reorganization at the interface and the subsequent adsorption of the enzyme onto the lipid monolayer. The evolution of the surface pressure and ellipsometric angle after injection of gastric lipase in the subphase of the GL/DPPC system (fig. 2.B) followed a similar evolution. The maximum increase in the surface pressure ($\Delta\pi_{max}$) was similar for both systems ($\Delta\pi_{max}$=1.2 mN/m vs 1.4 mN/m, for GL and GL/DPPC films, respectively). Nevertheless, for the $GL_{50}/DPPC_{50}$

monolayer, the ellipsometric angle started to increase right after the injection of the lipase into the subphase, reflecting a faster adsorption of the rDGL onto the heterogeneous film, probably due to the different orientation of the GL polar heads in the presence of DPPC. Indeed, the lag phase before the start of rDGL adsorption observed in the case of the GL monolayer could be due to the packing and orientation of the GL polar heads, which could hinder the access of the enzyme active site to the interface. In addition, it is important to point that addition of DPPC triggers phase separation which has been demonstrated as a structural feature favoring rDGL adsorption. For both systems, an equilibrium plateau was reached from 3h and until the end of the kinetics, with similar values for both GL and GL/DPPC systems ($\delta\Delta=10.5 \pm 0.5°$).

The $\Delta\pi_{max}$ values obtained upon rDGL adsorption on GL and GL/DPPC films are lower than those previously recorded upon rDGL adsorption onto pure phospholipid (PC) films (Bénarouche et al., 2017) or films mimicking bovine milk fat membranes and presenting phases coexistence (Bourlieu et al., 2016). This may result from weaker electrostatic interactions of rDGL with the neutral GL (compared to milk polar lipids (MPL)) which in general have charged polar heads. In addition to weaker electrostatic interactions, the galactose residues of GL polar heads may also generate some steric hindrance for lipase penetration into the film. Difference in fatty acyl moieties (chain length and unsaturation degree) may also influence lipid packing and rDGL adsorption.

3.2. Visualization of lipase organization into galactolipid monolayers by atomic force microscopy

AFM images of monomolecular films in the presence of rDGL were made after sampling the interface using the Langmuir Blodgett method after 2h of kinetics. The use of AFM allowed the topographic visualization of the interface at the nanoscopic scale. The AFM images of the interface were compared before and after the rDGL injection to highlight the distribution of the enzyme in the GL films and to determine the reorganization of the monolayers induced by the lipid-protein interactions. Details on AFM study on GL mixed films in the absence of rDGL are reported in Kergomard et al. (2022).

The injection of rDGL in the subphase (40 nM) clearly modified the morphology of the GL film (Figure 3) and triggered the formation of homogeneous patches onto the fluid phase after 2h of kinetics. These patches, assumed to reflect protein adsorption, had a mean width of 300 nm, which could correspond to 60 rDGL molecules, taking a width of about 5 nm for a rDGL molecule (Bénarouche et al., 2013). The roughness of the GL film before the enzyme injection was no longer visible on the AFM images in the presence of rDGL, suggesting a modification of the galactolipid-galactolipid interactions as well as a reorganization of the galactolipid polar heads induced by the adsorption of the rDGL onto the lipid film. Based on the analysis of five sections of the AFM image, the height variations of the fluid lipid background ranged from 0 to 0.5 nm (average height=0.24 ± 0.12 nm), representing about 57% of the interfacial film. After rDGL adsorption, the cross-section profiles of the AFM images displayed several peaks of varying heights and were divided into two categories depending on their height levels and occurrences. A first height level was identified, with peaks ranging from 0.5 to 2.0 nm (average height=0.98 ± 0.4 nm), accounting for 17% of the interfacial film. A second level was also detected, with heights ranging from 2.0 nm

to 5.5 nm (average height=4.0 ± 0.8 nm), representing about 26% of the interface on the AFM image. On this second height population, 55% of the heights were included between 3.9 and 4.5 nm, which could correspond to the entire cross-section of rDGL molecules (Roussel et al., 2002) and thus of protein patches covering an average area of 336 nm² (15 pixels per AFM image), which would correspond to a consistent value of 47 rDGL molecules, taking a cross-sectional area of 7.2 nm² at 20 mN/m, as reported by (Bénarouche et al., 2013).

3.3. Visualization of lipase organization into galactolipid-phospholipids monolayers by atomic force microscopy

A saturated phospholipid (DPPC) was added at a molar ratio of 50% in the GL mixture, in order to induce phase heterogeneity and determine the impact of such heterogeneity on the rDGL adsorption by introduction of a liquid condensed phase (LC) in the monolayer. The AFM images (5×5 µm² and 2.5×2.5 µm²) of the interfacial film before and after the injection of the rDGL in the subphase of the GL/DPPC monolayer are presented Figure 4.A.

After injection of the enzyme, the LC domains have merged, adopting a more circular shape, with heights of 1.7 to 2.3 nm (average height=1.8 ± 0.1 nm), covering an average surface of 36% of the interfacial film. At the very center and on the sides of the LC domains, bright peaks of 2.0 to 8.0 nm in height were also visible, circularly distributed, pointing the heterogeneity of the gel phase domains. Onto the fluid phase (LE), an irregular protein network was formed, much denser than the one observed in the case of the GL film (fig. 3), and made of small grains forming interconnected units of 50.0 ± 20.0 nm width. A sharp demarcation was also visible between the protein network in the fluid phase and the condensed domains, indicating rDGL exclusion from the LC-LE phase boundary and LC domains.

Size analyses and thresholds on AFM images led to the identification of height levels induced by the interactions of rDGL with the heterogeneous membrane, which are summarized Table 2. As for the GL monolayer, two different height profiles were identified at the fluid phase level, with similar profiles, indicating the preferential adsorption of the enzyme at the level of the fluid phase. A new higher height profile was identified at the level of the condensed domains, where the lipase probably has more difficulty to adsorb due to the high packing.

3.4. Impact of phytosterol addition in galactolipid-phospholipids mixture on the adsorption behavior of the gastric lipase

The inclusion of phytosterols in the GL/DPPC mixture has been shown to generate defects at the level of the condensed phase, due to the preferential interactions between the phytosterols and the saturated fatty acids (Kergomard et al. (2022)). The AFM images Figure 4.B revealed that 2h after the injection of rDGL into the subphase, a regular protein network has formed onto the fluid phase. This network is composed of interconnected units of the same width as the protein network formed at the interface of the GL film (30.0 ± 0.0 nm), suggesting a similar organization of the proteins. Additionally, the delineation between the fluid phase protein network and the condensed phase domains was no longer visible on the AFM images, in contrast to the $GL_{50}/DPPC_{50}$ film, indicating a modification of the protein-lipid interactions and probably a better miscibility of the components at the interface when pS were added in the system. As for the two previous samples, image and size analyses have revealed different levels of rDGL adsorption on the lipid film, which are reported Table 2.

4 DISCUSSION

rDGL has been shown to exhibit a high affinity for the air/water or lipid/water interface covered by polar lipids and to form monolayers, which distinguishes it from other globular proteins that tend to form multilayers (Bolanos-Garcia et al., 2008; Bourlieu et al., 2016). The formation of a monolayer was also deduced from rDGL adsorption onto a siliconized hydrophobic surface, monitored using a quartz crystal microbalance (Chahinian et al., 2006). This is probably due to its structural adaptation that avoids interfacial denaturation and involves a localized conformation change (lid opening) with the formation of an IRS on one side of the molecule (Figure 1) (Mateos-Diaz et al., 2017). The binding capacity of the rDGL at the air/water interface was monitored as the increase in the surface pressure π_{max}, correlated to the variations of the lipid packing and the adsorption of enzyme molecules onto the monolayer. Here, the combination of data obtained with ellipsometry, tensiometry, and atomic force microscopy analyses provided insights on the physicochemical behavior and the distribution of rDGL in mixed GL films at the air/water interface.

4.1. The particular orientation of the galactolipid polar heads could limit the enzyme adsorption at the interface of the monolayer despite the high surface activity of rDGL

The adsorption of rDGL onto mixed GL film (initial π=20 mN/m) triggered a slight increase in the surface pressure ($\Delta\pi_{max}$=1.2 mN/m). Although this result reflects lipid-protein interactions at the air-water interface, this increase in the surface pressure was more discrete than those reported by Bottier (2006) upon the adsorption of pin-a isoform of puroindoline, a small globular protein (13 kDa), onto homogenous monolayers of pure MGDG or DGDG isolated from wheat. Indeed, a pressure increase of 4.4 and 2.5 mN/m at 20 mN/m was obtained upon adsorption of pin-a onto

pure MGDG and DGDG films, respectively. The insertion of pin-a onto the GL films could be explained by the fluidity of GL as well as by the establishment of hydrophobic and Van der Walls interactions between the galactosyl head groups and the numerous tryptophan moieties of puroindolines, favoring their penetration into GL films. Furthermore, the overlap of the MGDG heads from 20 mN/m could have induced the formation of local instabilities, favoring the insertion of the protein in the film, explaining the greater increase of pressure. Conversely, the larger polar heads of DGDG could have limited the insertion of pin-a, thus explaining the lower pressure increase. Indeed, despite the larger polar head of DGDG than MGDG, digalactosyl residues possess the ability to adopt a tilted orientation, at 40° to the interface normal, in contrast to the polar head of pure MGDG, which was oriented parallel to the interface (Bottier, 2006). The particular orientation of the digalactosyl residue of DGDG is consistent with the results obtained by Chu et al. (2010) on the digestibility of an olive oil stabilized by either DPPC or DGDG, showing that the air/water interface occupied by DGDG was more resistant to the adsorption of bile salts, pancreatic lipase and colipase compared to the interface occupied by DPPC.

The small increase in surface pressure and the latency phase observed before the increase of the ellipsometric angle in the case of rDGL is therefore more consistent with a discrete adsorption behavior onto the mixed GL monolayers at 20 mN/m. The more limited insertion of rDGL could have been due to the larger size of the protein (50 kDa versus 13 kDa for pin-a puroindoline), but also to the fact that the monolayer was composed of a mixture of GL, and not of pure MGDG or DGDG. Indeed, in the equimolar mixture, a reorientation of the DGDG polar heads was observed, with the digalactosyl moiety orienting parallel to the interface, suggesting strong interactions between MGDG and DGDG and allowing tighter packing of mixed galactolipid molecules at the interface that could inhibit the lipase adsorption (Bottier, 2006). Moreover, the adsorption kinetics

properties of gastric lipase could also result from the interactions between the substrates and the active site of the enzyme. The IRS of rDGL being composed of several basic residues (Figure 1.C), it is less likely to develop electrostatic interactions with an uncharged galactolipid monolayer than with a charged phospholipid monolayer. This feature probably explains the lower adsorption capacity of rDGL to GL monolayer. The absence of charge at an interface decreases the establishment of electrostatic interactions with the enzyme, which could slow down or even hinder its adsorption.

Overall, the extend of rDGL adsorption onto the lipid monolayer seems to be highly dependent on the lipid packing and acyl chain composition. Indeed, a higher increase of π ($\Delta\pi_{max}$=8 mN/m) was reported for the rDGL adsorption onto 1,2-dilauroyl-sn-glycero-3-phosphocholine (DLPC) monolayer in the same conditions (Bénarouche et al., 2013). Moreover, rDGL shows a higher penetration capacity into medium chain DLPC than into long chain egg PC monolayers, with critical surface pressures of insertion (π_c) of 30.3 mN/m and 21.5 mN/m, respectively. The surface pressure chosen here with GL film (π=20 mN/m) therefore represents harsh conditions for rDGL adsorption and penetration. An higher increase of the surface pressure was also reported by Bourlieu et al. (2016) on milk polar lipids with or without residual triacylglycerols MPL and MPL_{TC} ($\Delta\pi_{max}$=2.4 mN/m and $\Delta\pi_{max}$=6.1 mN/m, respectively).

In our study, the ellipsometric data suggested that a significant amount of rDGL was adsorbed onto the GL monolayer after 1h latency phase, with a high ellipsometric angle variation of $\delta\Delta$=4.2° obtained after 2h of kinetics. This value was higher than that obtained on MPL ($\delta\Delta$=3.1°) but much lower ($\delta\Delta$=18.3°) than that obtained on MPL_{TC} after 5 hours of kinetics. Overall, the results of tensiometry and ellipsometry analysis confirmed the adsorption of rDGL onto the GL monolayer,

although to a lesser extent than for bovine milk membranes (MPL and MPL_{TC}) due to the particular orientation of the polar head of galactolipids and the uncharged surface of the monolayer.

4.2. rDGL undergoes conformational changes upon adsorption, explaining the different level of adsorption/insertion onto the GL films

The AFM images of the GL film evidenced the formation of protein patches at two different height levels in the fluid phase 2h after the injection of rDGL in the subphase. Different levels of rDGL adsorption have already been reported (Bénarouche et al., 2013, 2017; Bourlieu et al., 2016, 2020) as being dependent on the monolayer composition but also on the conformation of the adsorbed enzyme, which reflect its level of interaction and activity with the substrate. This may result from structural changes occurring upon protein adsorption at the air/water (or lipid/water) interface. The unfolding and denaturation of proteins at the interfaces are well-known behaviors, especially when interfacial tension is high. For example, lipases are rapidly inactivated at the oil-water interface when using pure triacylglycerols (Aloulou et al., 2006). Nevertheless, denaturation can be avoided using surfactants decreasing the interfacial tension or by the enzyme itself. Lipases like gastric lipase are also known to undergo a localized conformational change with a lid opening that controls the interfacial recognition site and activity (Mateos-Diaz et al., 2017). Coagulation/aggregation are additional phenomena that may also occur with proteins at interfaces (James & Augenstein, 1966). All these phenomena were likely to explain the different levels of insertion of the rDGL in the mixed GL film. Indeed, the lowest height level could correspond to some denatured rDGL, unfolded upon adsorption and resulting in an increase in the surface pressure, more favorable to the adsorption of the enzyme in its active conformation. The second height level corresponding to homogeneous peak sizes between 2.0 and 5.5 nm is likely to correspond to the adsorption of rDGL

in its active conformation, at a depth of 1 to 2 nm in the GL monolayer onto the GL monolayer at the air/water interface. This level of rDGL would fit with the adsorption model previously proposed for rDGL (Bénarouche et al., 2013). A model for the rDGL distribution in the GL monolayer under gastric conditions is proposed Figure 5.

4.3. rDGL is excluded from condensed phase domains in mixed heterogeneous GL-DPPC systems and exhibits similar adsorption behavior to other small globular proteins

Numerous studies have been conducted in AFM to investigate the adsorption of various lipases and phospholipases onto heterogenous supported monolayers and bilayers at the air/water interface (Balashev et al., 2007; Rangl et al., 2017). Overall, results have indicated the preferential adsorption of these enzymes at the edges of low molecular packing domains, where the increase of the curvature favor the amphiphile adsorption (Nielsen et al., 1999; Prim et al., 2006).

The lateral distribution of the gastric lipase in monolayers of milk fat globules with phase heterogeneity has been studied in both human and bovine systems (Bourlieu et al., 2016, 2020). The coexistence of liquid condensed/liquid expanded (LC/LE) phases in milk fat globule monolayers has been shown to impact the adsorption of gastric lipase. Indeed, the rDGL gets really rapidly adsorbed in the LE phase or at the phase boundaries in the bovine milk membrane (BMM) and human milk membrane (HMM) extracts, showing that the coexistence of LC/LE phase was an important driver of the rDGL adsorption.

Here, we introduced some phase heterogeneity in the GL monolayer by adding DPPC. As expected, the AFM images (fig. 4.A) revealed that the rDGL was excluded from the LC phase, and preferentially adsorb onto the LE phase of GL-DPPC monolayer, which present a lower molecular packing, probably due to the high composition in PUFA of GL. Indeed, the condensed domains

were likely to include DPPC, with tight packing of its saturated acyl chains preventing lipase penetration. Nevertheless, the bright peaks visible in the center of the condensed domains seemed to indicate an adsorption of rDGL at this level, probably due to some compositional heterogeneity between the center and the edge of the LC domains, favoring a less dense packing or the appearance of defects at the central level. On the other hand, the adsorption of the rDGL onto the LE phase triggered the formation of a dense protein network, composed by small interconnected nanodomains of irregular shape and width, in contrast to the discontinuous homogeneous network previously formed in the GL film. Several levels of rDGL insertions were identified, in line with the results of Bourlieu et al. (2016) on bovine milk fat model membranes (MPL and MPL_{TC}), with slightly different height values in those different heterogenous systems, which could be explain by the differences of composition and lipid packing between the monolayers.

Additionally, the condensed domains composing the LC phase merged and their circularity was increased, indicating the existence of a line tension at the interface of the LC/LE phases. Indeed, García-Sáez et al. (2007) have shown that the size and the shape of LC domains composed by sphingomyelin and cholesterol depend on the balance between the line tension, which tends to increase the size of the domains in order to reduce the total length of the boundaries, and the entropic and electrostatic repulsions, which prevent the fusion of the LC domains. Thus, the increase of the LC domain size in our study is consistent with a higher line tension at their edges. This change in line tension could be triggered by the greater height difference between the two phases LC and LE, induced by the adsorption of rDGL onto the fluid phase. Indeed, this height difference has an unfavorable energy cut per unit length, and as a result, the domain boundary deforms to counteract this phenomenon, inducing line tension, which may be unfavorable for rDGL adsorption. Indeed, the sharp domain delineation visible on the AFM image between the fluid-

phase protein network and the LC domains seems to indicate that the rDGL poorly adsorbs at the phase boundaries.

The adsorption behavior of rDGL on heterogeneous lipid films from animal or plant sources can be compared to other globular proteins. Weise et al. (2010) studied the adsorption behavior of several lipid membrane proteins, including N-Ras, a small globular protein (21 kDa), onto heterogeneous model membranes with coexisting fluid/gel phases. The results of this study provided direct evidence of the preferential distribution of the N-Ras protein in the fluid phase, but also at the edges of the LC phase domains, leading to a favorable decrease of the energy between the phases. This adsorption of proteins at boundary phases was characteristic of proteins inserted into multiphase lipid systems but which do not show specific preferences for a given phase, so that they are expelled toward the boundaries. This localization and accumulation of proteins at the phase interface to decrease the line tension could explain the adsorption behavior of rDGL in the presence of pS.

4.4. The addition of pS modulated the rDGL adsorption onto mixed GL-DPPC monolayers at the air/water interface

In our previous study, the inclusion of phytosterols (pS) in the GL/DPPC film induced a drastic modification of the interfacial organization, with a dilution of the domains as well as an increase in the thickness of the condensed phases. This was attributed to interactions between GL and PL and a condensation effect of pS (Li et al., 2003; Su et al., 2007). Moreover, the addition of pS to mixed DPPC and GL monolayers was found to trigger the appearance of defects into the condensed phase domains. Previous studies on various other lipases found that defects in lipid packing could constituted preferential sites for the enzyme anchoring (Balashev et al., 2001, 2007; Brezesinski & Möhwald, 2003; Nielsen et al., 2002). The presence of local defects in the LC phase GL/DPPC/pS

film reflects a less dense molecular packing, which could favor rDGL adsorption. Indeed, AFM images recorded after rDGL injection in the subphase of the films revealed significant differences in the organization at the interface between GL/DPPC and GL/DPPC/pS films. In the presence of pS, a regular protein network was visible on the AFM images, not only at the fluid phase but also at the phase domain boundaries and at the defects present on the condensed phase domains. The absence of a marked delineation of the protein network level between the LE and LC phases contrasts with the system without pS. It points to an enhancement of the rDGL adsorption onto the LC domains and at the boundary phase, leading to a decrease of the height difference between the LC/LE phases and thus to a decrease of the line tension (fig. 4.B), favoring a more homogenous adsorption of rDGL at the interface. This modulation of rDGL adsorption in the presence of pS could also be explained by a modification of the lipid-lipid and protein-lipid interactions. Indeed, hydrogen bridges could be established with the hydroxyl groups of pS, as well as stacking between rDGL aromatic residues and the sterol backbone, leading to a different interfacial organization and favoring the rDGL adsorption.

Moreover, the two different levels of rDGL insertion with homogeneous peak sizes onto the GL-DPPC-pS film (h2, h3) were comparable to those identified in the case of rDGL adsorption onto models of HMM by Bourlieu et al. (2020). In contrast, rDGL insertion onto BMM was less homogeneous, with 3 levels of heights described, similar to the ones evidenced for the GL-DPPC film. It was speculated by the authors that the particular composition of HMM (high PUFA content, presence of DHA, presence of anionic PL, coexistence of LC/LE phase) was more favorable to the action of rDGL than the composition of BMM. Indeed, HMM contained more anionic phospholipids, which have been shown to enhance the adsorption of rDGL at pH 5 thanks to a better reorientation of the charged active site.

Interest of the study for the adsorption of gastric lipase onto natural plant cell membranes

Plant cell membranes are complex systems containing a large variety of lipid and protein molecules. The high proportion of DPPC in our model systems (50%) was explained by the need to create a heterogeneous system, presenting a coexistence of LC/LE phase observable in AFM, but was actually far from the palmitic acid compositions (C16 :0) found in natural plant membrane systems (plasma membrane, chloroplast thylakoids, oleosomes) (Kergomard et al., 2021). Indeed, the proportion of palmitoyl chains in natural plant systems is on average between 5-20% wt. of total lipids (Lee et al., 1998; Venkatachalam & Sathe, 2006). Nevertheless, the raft theory in plant membrane systems predicts the existence of lipid assemblies locally enriched in phytosterol and sphingolipid molecules (Mongrand et al., 2010), which are known to contain liquid-ordered domains in a fluid environment (Bhat & Panstruga, 2005). These plant membrane rafts are biochemical homologues of mammalian cell membrane rafts rich in sphingomyelin and cholesterol, known for their transient dynamic structure in the nanometer range and involved in signaling and protein transport processes and other cellular processes (Hancock, 2006; Jacobson et al., 2007; Munro, 2003).

Thus, although our biomimetic membranes constituted a simplified model somewhat far from the natural plant membrane composition, the general physicochemical trends and adsorption behavior of gastric lipase at these heterogeneous model membrane systems remain extendable to the protein-lipid interactions occurring at the so-called raft zones in plant cells. In particular, it appeared that the presence of phytosterols in condensed domains and, by extension, in plant rafts, may enhance the rDGL adsorption at Lo or gel phase (LC) domains.

CONCLUSION

We have shown that Langmuir films and their analysis by tensiometry, ellipsometry and Langmuir-Blodgett transfer coupled to atomic force microscopy provide a suitable tool for studying the adsorption and interactions of gastric lipase with biomimetic vegetal membranes. Gastric lipase binds to these heterogenous membranes with a preference for phase boundaries and defects. It induces changes in the interfacial organization of lipids although it does not display any activity on polar acylglycerols from plant membranes (Wattanakul et al., 2019). Since gastric lipase is known to promote the action of pancreatic lipase through the release of fatty acids and changes in interfacial properties (Gargouri et al., 1986), the changes observed with plant polar lipids, without lipolysis, may also trigger the adsorption and activity of other pancreatic enzymes. This will be the objective of further studies, but the present one is a step forward in the comprehension of gastrointestinal lipase interactions with plant membranes, an overlooked aspect of lipid digestion (Sahaka et al., 2020).

Declaration of Competing Interest

The authors declare that they have no known competing financial interests or personal relationships that could have appeared to influence the work reported in this paper.

Acknowledgments

The authors would like to acknowledge the BIOMIF platform ('Biological Molecules at fluid interfaces', IPR, Rennes, France) for allowing the biophysical characterization of samples presented in this article.

C. Bourlieu, V. Vié and J. Kergomard determined the outline and the content of the manuscript. J. Kergomard wrote the manuscript and all the co-authors participated in the experimental design, the collection, the interpretation of data and the correction and implementation of the manuscript. All co-authors have approved the final article.

References

Aloulou, A., Rodriguez, J. A., Fernandez, S., van Oosterhout, D., Puccinelli, D., & Carrière, F. (2006). Exploring the specific features of interfacial enzymology based on lipase studies. *Biochimica et Biophysica Acta (BBA) - Molecular and Cell Biology of Lipids*, *1761*(9), 995-1013. https://doi.org/10.1016/j.bbalip.2006.06.009

Balashev, K., Jensen, T. R., Kjaer, K., & Bjørnholm, T. (2001). Novel methods for studying lipids and lipases and their mutual interaction at interfaces. Part I. Atomic force microscopy. *Biochimie*, *83*(5), 387-397. https://doi.org/10.1016/S0300-9084(01)01264-0

Balashev, K., John DiNardo, N., Callisen, T. H., Svendsen, A., & Bjørnholm, T. (2007). Atomic force microscope visualization of lipid bilayer degradation due to action of phospholipase A2 and Humicola lanuginosa lipase. *Biochimica et Biophysica Acta (BBA) - Biomembranes*, *1768*(1), 90-99. https://doi.org/10.1016/j.bbamem.2006.09.028

Bénarouche, A., Point, V., Parsiegla, G., Carrière, F., & Cavalier, J.-F. (2013). New insights into the pH-dependent interfacial adsorption of dog gastric lipase using the monolayer technique. *Colloids and Surfaces B: Biointerfaces*, *111*, 306-312. https://doi.org/10.1016/j.colsurfb.2013.06.025

Bénarouche, A., Sams, L., Bourlieu, C., Vié, V., Point, V., Cavalier, J. F., & Carrière, F. (2017). Chapter Eleven—Studying Gastric Lipase Adsorption Onto Phospholipid Monolayers by Surface Tensiometry, Ellipsometry, and Atomic Force Microscopy. In M. H. Gelb (Éd.), *Methods in Enzymology* (Vol. 583, p. 255-278). Academic Press. https://doi.org/10.1016/bs.mie.2016.09.039

Berge, B., & Renault, A. (1993). Ellipsometry Study of 2D Crystallization of 1-Alcohol Monolayers at the Water Surface. *Europhysics Letters (EPL), 21*(7), 773-777. https://doi.org/10.1209/0295-5075/21/7/010

Bhat, R. A., & Panstruga, R. (2005). Lipid rafts in plants. *Planta*, *223*(1), 5. https://doi.org/10.1007/s00425-005-0096-9

Bolanos-Garcia, V. M., Renault, A., & Beaufils, S. (2008). Surface Rheology and Adsorption Kinetics Reveal the Relative Amphiphilicity, Interfacial Activity, and Stability of Human Exchangeable Apolipoproteins. *Biophysical Journal*, *94*(5), 1735-1745. https://doi.org/10.1529/biophysj.107.115220

Bottier, C. (2006). *Caractérisation des puroindolines, des galactolipides du blé et de leurs interactions : Mesures physiques aux interfaces* [Phdthesis, Université Rennes 1]. https://tel.archives-ouvertes.fr/tel-00148405

Bourlieu, C., Mahdoueni, W., Paboeuf, G., Gicquel, E., Ménard, O., Pezennec, S., Bouhallab, S., Deglaire, A., Dupont, D., Carrière, F., & Vié, V. (2020). Physico-chemical behaviors of human and bovine milk membrane extracts and their influence on gastric lipase adsorption. *Biochimie*, *169*, 95-105. https://doi.org/10.1016/j.biochi.2019.12.003

Bourlieu, C., Ménard, O., De La Chevasnerie, A., Sams, L., Rousseau, F., Madec, M.-N., Robert, B., Deglaire, A., Pezennec, S., Bouhallab, S., Carrière, F., & Dupont, D. (2015). The structure of infant formulas impacts their lipolysis, proteolysis and disintegration during in vitro gastric digestion. *Food Chemistry*, *182*, 224-235. https://doi.org/10.1016/j.foodchem.2015.03.001

Bourlieu, C., Paboeuf, G., Chever, S., Pezennec, S., Cavalier, J.-F., Guyomarc'h, F., Deglaire, A., Bouhallab, S., Dupont, D., Carrière, F., & Vié, V. (2016). Adsorption of gastric lipase onto

multicomponent model lipid monolayers with phase separation. *Colloids and Surfaces B: Biointerfaces, 143*, 97-106. https://doi.org/10.1016/j.colsurfb.2016.03.032

Brezesinski, G., & Möhwald, H. (2003). Langmuir monolayers to study interactions at model membrane surfaces. *Advances in Colloid and Interface Science, 100-102*, 563-584. https://doi.org/10.1016/S0001-8686(02)00071-4

Canaan, S., Roussel, A., Verger, R., & Cambillau, C. (1999). Gastric lipase : Crystal structure and activity. *Biochimica et Biophysica Acta (BBA) - Molecular and Cell Biology of Lipids, 1441*(2), 197-204. https://doi.org/10.1016/S1388-1981(99)00160-2

Cañabate-Díaz, B., Segura Carretero, A., Fernández-Gutiérrez, A., Belmonte Vega, A., Garrido Frenich, A., Martínez Vidal, J. L., & Duran Martos, J. (2007). Separation and determination of sterols in olive oil by HPLC-MS. *Food Chemistry, 102*(3), 593-598. https://doi.org/10.1016/j.foodchem.2006.05.038

Carrière, F., Moreau, H., Raphel, V., Laugier, R., Benicourt, C., Junien, J. L., & Verger, R. (1991). Purification and biochemical characterization of dog gastric lipase. *European Journal of Biochemistry, 202*(1), 75-83. https://doi.org/10.1111/j.1432-1033.1991.tb16346.x

Carrière, F., Renou, C., Ransac, S., Lopez, V., De Caro, J., Ferrato, F., De Caro, A., Fleury, A., Sanwald-Ducray, P., Lengsfeld, H., Beglinger, C., Hadvary, P., Verger, R., & Laugier, R. (2001). Inhibition of gastrointestinal lipolysis by Orlistat during digestion of test meals in healthy volunteers. *American Journal of Physiology-Gastrointestinal and Liver Physiology, 281*(1), G16-G28. https://doi.org/10.1152/ajpgi.2001.281.1.G16

Chahinian, H., Snabe, T., Attias, C., Fojan, P., Petersen, S. B., & Carrière, F. (2006). How Gastric Lipase, an Interfacial Enzyme with a Ser-His-Asp Catalytic Triad, Acts Optimally at Acidic pH. *Biochemistry, 45*(3), 993-1001. https://doi.org/10.1021/bi0518803

Chu, B.-S., Gunning, A. P., Rich, G. T., Ridout, M. J., Faulks, R. M., Wickham, M. S. J., Morris, V. J., & Wilde, P. J. (2010). Adsorption of Bile Salts and Pancreatic Colipase and Lipase onto Digalactosyldiacylglycerol and Dipalmitoylphosphatidylcholine Monolayers. *Langmuir*, *26*(12), 9782-9793. https://doi.org/10.1021/la1000446

de La Fournière, L., Ivanova, M. G., Blond, J.-P., Carrière, F., & Verger, R. (1994). Surface behaviour of human pancreatic and gastric lipases. *Colloids and Surfaces B: Biointerfaces*, *2*(6), 585-593. https://doi.org/10.1016/0927-7765(94)80069-3

Dörmann, P., & Benning, C. (2002). Galactolipids rule in seed plants. *Trends in Plant Science*, *7*(3), 112-118. https://doi.org/10.1016/S1360-1385(01)02216-6

Dufourc, E. J. (2008). The role of phytosterols in plant adaptation to temperature. *Plant Signaling & Behavior*, *3*(2), 133-134. https://doi.org/10.4161/psb.3.2.5051

García-Sáez, A. J., Chiantia, S., & Schwille, P. (2007). Effect of line tension on the lateral organization of lipid membranes. *The Journal of Biological Chemistry*, *282*(46), 33537-33544. https://doi.org/10.1074/jbc.M706162200

Gargouri, Y., Pieroni, G., Rivière, C., Lowe, P. A., Saunière, J. F., Sarda, L., & Verger, R. (1986). Importance of human gastric lipase for intestinal lipolysis : An in vitro study. *Biochimica Et Biophysica Acta*, *879*(3), 419-423. https://doi.org/10.1016/0005-2760(86)90234-1

Grosjean, K., Mongrand, S., Beney, L., Simon-Plas, F., & Gerbeau-Pissot, P. (2015). Differential Effect of Plant Lipids on Membrane Organization : SPECIFICITIES OF PHYTOSPHINGOLIPIDS AND PHYTOSTEROLS*. *Journal of Biological Chemistry*, *290*(9), 5810-5825. https://doi.org/10.1074/jbc.M114.598805

Hąc-Wydro, K., Wydro, P., Jagoda, A., & Kapusta, J. (2007). The study on the interaction between phytosterols and phospholipids in model membranes. *Chemistry and Physics of Lipids*, *150*(1), 22-34. https://doi.org/10.1016/j.chemphyslip.2007.06.211

650 Hancock, J. F. (2006). Lipid rafts : Contentious only from simplistic standpoints. *Nature Reviews.*
651 *Molecular Cell Biology*, *7*(6), 456-462. https://doi.org/10.1038/nrm1925
652 Huang, A. H. C. (1987). 4—Lipases. In P. K. Stumpf (Éd.), *Lipids : Structure and Function* (Vol.
653 9, p. 91-119). Academic Press. https://doi.org/10.1016/B978-0-12-675409-4.50010-1
654 Ikekawa, N., Morisaki, N., Tsuda, K., & Yoshida, T. (1968). Sterol compositions in some green
655 algae and brown algae. *Steroids*, *12*(1), 41-48. https://doi.org/10.1016/S0039-
656 128X(68)80078-9
657 Infantes-Garcia, M. R., Verkempinck, S. H. E., Hendrickx, M. E., & Grauwet, T. (2021). Kinetic
658 Modeling of In Vitro Small Intestinal Lipid Digestion as Affected by the Emulsion
659 Interfacial Composition and Gastric Prelipolysis. *Journal of Agricultural and Food*
660 *Chemistry*, *69*(16), 4708-4719. https://doi.org/10.1021/acs.jafc.1c00432
661 Itoh, T., Tamura, T., Matsumoto, T., & Surugadai, K. (1973). *Sterol composition of 19 vegetable*
662 *oils*. 4.
663 Jacobson, K., Mouritsen, O. G., & Anderson, R. G. W. (2007). Lipid rafts : At a crossroad between
664 cell biology and physics. *Nature Cell Biology*, *9*(1), 7-14. https://doi.org/10.1038/ncb0107-
665 7
666 Jaeger, K. E., Ransac, S., Dijkstra, B. W., Colson, C., van Heuvel, M., & Misset, O. (1994).
667 Bacterial lipases. *FEMS Microbiology Reviews*, *15*(1), 29-63.
668 https://doi.org/10.1111/j.1574-6976.1994.tb00121.x
669 James, L. K., & Augenstein, L. G. (1966). Adsorption of enzymes at interfaces : Film formation
670 and the effect on activity. *Advances in Enzymology and Related Areas of Molecular*
671 *Biology*, *28*, 1-40. https://doi.org/10.1002/9780470122730.ch1
672 Kergomard, J., Carrière, F., Barouh, N., Villeneuve, P., Vié, V., & Bourlieu, C. (2021).
673 Digestibility and oxidative stability of plant lipid assemblies : An underexplored source of

potentially bioactive surfactants? *Critical Reviews in Food Science and Nutrition*, 1-20. https://doi.org/10.1080/10408398.2021.2005532

Kergomard, J., Carrière, F., Paboeuf, G., Artzner, F., Barouh, N., Bourlieu, C., & Vié, V. (2022). Interfacial organization and phase behavior of mixed galactolipid-DPPC-phytosterol assemblies at the air-water interface and in hydrated mesophases. *Colloids and Surfaces B: Biointerfaces*, 112646. https://doi.org/10.1016/j.colsurfb.2022.112646

Lee, D.-S., Noh, B.-S., Bae, S.-Y., & Kim, K. (1998). Characterization of fatty acids composition in vegetable oils by gas chromatography and chemometrics. *Analytica Chimica Acta*, *358*(2), 163-175. https://doi.org/10.1016/S0003-2670(97)00574-6

Lengsfeld, H., Beaumier-Gallon, G., Chahinian, H., De Caro, A., Verger, R., Laugier, R., & Carrière, F. (2004). Physiology of Gastrointestinal Lipolysis and Therapeutical Use of Lipases and Digestive Lipase Inhibitors. In *Lipases and Phospholipases in Drug Development* (p. 195-229). John Wiley & Sons, Ltd. https://doi.org/10.1002/3527601910.ch10

Lerique, B., Lepetit-Thévenin, J., Vérine, A., Delpéro, C., & Boyer, J. (1994). Triacylglycerol in biomembranes. *Life Sciences*, *54*(13), 831-840. https://doi.org/10.1016/0024-3205(94)00619-9

Li, X.-M., Momsen, M. M., Brockman, H. L., & Brown, R. E. (2003). Sterol Structure and Sphingomyelin Acyl Chain Length Modulate Lateral Packing Elasticity and Detergent Solubility in Model Membranes. *Biophysical Journal*, *85*(6), 3788-3801.

Mateos-Diaz, E., Amara, S., Roussel, A., Longhi, S., Cambillau, C., & Carrière, F. (2017). Probing Conformational Changes and Interfacial Recognition Site of Lipases With Surfactants and Inhibitors. *Methods in Enzymology*, *583*, 279-307. https://doi.org/10.1016/bs.mie.2016.09.040

Moghadasian, M. H., & Frohlich, J. J. (1999). Effects of dietary phytosterols on cholesterol metabolism and atherosclerosis : Clinical and experimental evidence. *The American Journal of Medicine*, *107*(6), 588-594. https://doi.org/10.1016/S0002-9343(99)00285-5

Mongrand, S., Stanislas, T., Bayer, E. M. F., Lherminier, J., & Simon-Plas, F. (2010). Membrane rafts in plant cells. *Trends in Plant Science*, *15*(12), 656-663. https://doi.org/10.1016/j.tplants.2010.09.003

Munro, S. (2003). Lipid Rafts : Elusive or Illusive? *Cell*, *115*(4), 377-388. https://doi.org/10.1016/S0092-8674(03)00882-1

Nicholls, A. J. (1993). *GRASP Manual*. Columbia University.

Nielsen, L. K., Balashev, K., Callisen, T. H., & Bjørnholm, T. (2002). Influence of product phase separation on phospholipase A(2) hydrolysis of supported phospholipid bilayers studied by force microscopy. *Biophysical Journal*, *83*(5), 2617-2624.

Nielsen, L. K., Risbo, J., Callisen, T. H., & Bjørnholm, T. (1999). Lag-burst kinetics in phospholipase A2 hydrolysis of DPPC bilayers visualized by atomic force microscopy. *Biochimica et Biophysica Acta (BBA) - Biomembranes*, *1420*(1), 266-271. https://doi.org/10.1016/S0005-2736(99)00103-0

Petersen, S. B., Fojan, P., Petersen, E. I., & Petersen, M. T. N. (2001). The thermal stability of the Fusarium solani pisi cutinase as a function of pH. *Journal of Biomedicine and Biotechnology*, *1*(2), 62-69. https://doi.org/10.1155/S1110724301000249

Phillips, K. M., Ruggio, D. M., & Ashraf-Khorassani, M. (2005). Phytosterol Composition of Nuts and Seeds Commonly Consumed in the United States. *Journal of Agricultural and Food Chemistry*, *53*(24), 9436-9445. https://doi.org/10.1021/jf051505h

Prim, N., Iversen, L., Diaz, P., & Bjørnholm, T. (2006). Atomic force microscope studies on the interactions of Candida rugosa lipase and supported lipidic bilayers. *Colloids and Surfaces B: Biointerfaces*, *52*(2), 138-142. https://doi.org/10.1016/j.colsurfb.2006.05.018

Rangl, M., Rima, L., Klement, J., Miyagi, A., Keller, S., & Scheuring, S. (2017). Real-time Visualization of Phospholipid Degradation by Outer Membrane Phospholipase A using High-Speed Atomic Force Microscopy. *Journal of Molecular Biology*, *429*(7), 977-986. https://doi.org/10.1016/j.jmb.2017.03.004

Roussel, A., Canaan, S., Egloff, M.-P., Rivière, M., Dupuis, L., Verger, R., & Cambillau, C. (1999). Crystal Structure of Human Gastric Lipase and Model of Lysosomal Acid Lipase, Two Lipolytic Enzymes of Medical Interest*. *Journal of Biological Chemistry*, *274*(24), 16995-17002. https://doi.org/10.1074/jbc.274.24.16995

Roussel, A., Miled, N., Berti-Dupuis, L., Rivière, M., Spinelli, S., Berna, P., Gruber, V., Verger, R., & Cambillau, C. (2002). Crystal Structure of the Open Form of Dog Gastric Lipase in Complex with a Phosphonate Inhibitor*. *Journal of Biological Chemistry*, *277*(3), 2266-2274. https://doi.org/10.1074/jbc.M109484200

Sahaka, M., Amara, S., Wattanakul, J., Gedi, M. A., Aldai, N., Parsiegla, G., Lecomte, J., Christeller, J. T., Gray, D., Gontero, B., Villeneuve, P., & Carrière, F. (2020). The digestion of galactolipids and its ubiquitous function in Nature for the uptake of the essential α-linolenic acid. *Food & Function*. https://doi.org/10.1039/D0FO01040E

Silva, C., Aranda, F. J., Ortiz, A., Carvajal, M., Martínez, V., & Teruel, J. A. (2007). Root Plasma Membrane Lipid Changes in Relation to Water Transport in Pepper : A Response to NaCl and CaCl2 Treatment. *Journal of Plant Biology*, *50*(6), 650-657. https://doi.org/10.1007/BF03030609

743 Silva, C., Aranda, F. J., Ortiz, A., Martínez, V., Carvajal, M., & Teruel, J. A. (2011). Molecular
744 aspects of the interaction between plants sterols and DPPC bilayers : An experimental and
745 theoretical approach. *Journal of Colloid and Interface Science*, *358*(1), 192-201.
746 https://doi.org/10.1016/j.jcis.2011.02.048
747 Silvius, J. R. (2005). Partitioning of membrane molecules between raft and non-raft domains :
748 Insights from model-membrane studies. *Biochimica et Biophysica Acta (BBA) - Molecular*
749 *Cell Research*, *1746*(3), 193-202. https://doi.org/10.1016/j.bbamcr.2005.09.003
750 Su, Y., Li, Q., Chen, L., & Yu, Z. (2007). Condensation effect of cholesterol, stigmasterol, and
751 sitosterol on dipalmitoylphosphatidylcholine in molecular monolayers. *Colloids and*
752 *Surfaces A: Physicochemical and Engineering Aspects*, *293*(1), 123-129.
753 https://doi.org/10.1016/j.colsurfa.2006.07.016
754 Venkatachalam, M., & Sathe, S. K. (2006). Chemical composition of selected edible nut seeds.
755 *Journal of Agricultural and Food Chemistry*, *54*(13), 4705-4714.
756 https://doi.org/10.1021/jf0606959
757 von Bergmann, K., Sudhop, T., & Lütjohann, D. (2005). Cholesterol and Plant Sterol Absorption :
758 Recent Insights. *The American Journal of Cardiology*, *96*(1, Supplement), 10-14.
759 https://doi.org/10.1016/j.amjcard.2005.03.014
760 Wattanakul, J., Sahaka, M., Amara, S., Mansor, S., Gontero, B., Carrière, F., & Gray, D. (2019).
761 In vitro digestion of galactolipids from chloroplast-rich fraction (CRF) of postharvest, pea
762 vine field residue (haulm) and spinach leaves. *Food & Function*, *10*(12), 7806-7817.
763 https://doi.org/10.1039/C9FO01867K
764 Weise, K., Triola, G., Janosch, S., Waldmann, H., & Winter, R. (2010). Visualizing association of
765 lipidated signaling proteins in heterogeneous membranes−Partitioning into subdomains,
766 lipid sorting, interfacial adsorption, and protein association. *Biochimica et Biophysica Acta*

767 *(BBA) - Biomembranes*, *1798*(7), 1409-1417.
768 https://doi.org/10.1016/j.bbamem.2009.12.006
769
770

FIGURES

Figure captions.

Figure 1 3D structure of recombinant dog gastric lipase showing the interfacial recognition site (IRS). Panel A: ribbon model showing the secondary structure elements of rDGL with the lid in the open conformation and putative orientation at lipid-water interface based on the localization of the IRS. Panel B*:* Top view and molecular surface representation (white=hydrophobic; yellow=polar) of rDGL showing the hydrophobic ring surrounding the active site entrance. Panel C: Top view and molecular surface representation showing its surface potential at pH 5 Surface potential scale is given below the rDGL structure, with red and blue colors corresponding to negative and positive potential, respectively. Views were prepared using PyMol software (Schrodinger, L. (2010) The PyMOL Molecular Graphics System, Version 1.3r1.) and the crystal structure of rDGL (PDB: 1K8Q). Surface potential was estimated using the TITRA software program (Petersen et al., 2001) and the protein surfaces were generated using GRASP (Nicholls, 1993).

Figure 2 (A) Kinetic evolution of the surface pressure (circle, red) and ellipsometric angle (triangle, blue) upon rDGL adsorption at the air/water interface onto GL lipid film and, (B) Kinetic evolution of the surface pressure (circle, red) and ellipsometric angle (triangle, blue) upon rDGL adsorption onto $GL_{50}/DPPC_{50}$ monolayers performed at an initial surface pressure of 20 mN/m. The rDGL was injected in the subphase after 5 minutes stabilization of the monolayers at the air/water interface.

Figure 3 AFM images (5×5 µm² and 1×1 µm²) of GL monolayers at an initial surface pressure of 20 mN/m before (-rDGL, red) and after (+rDGL, green) rDGL injection (40 nM final concentration, 5h kinetics). A cross-section of height profile is representative for 1x1 µm² image after rDGL

injection. ImageJ analysis was performed on a 0.56 µm² crop to determine the shape of the protein network (see material and methods). The vertical color scale from dark brown to white corresponds to an overall height of 15 nm.

Figure 4 AFM images (5×5 µm² and 2.5×2.5 µm²) at an initial surface pressure of 20 mN/m before (-rDGL, red) and after (+rDGL, green) rDGL injection (40 nM final concentration, 5h kinetics) of A) GL/DPPC monolayer (50:50 mol/mol) and B) GL/DPPC/pS monolayer (45:45:10 mol/mol/mol). Cross-sections of height profiles are representative for 2.5×2.5 µm² image after rDGL injection. (LE – Liquid Expended, fluid phase; LC – Liquid Condensed, gel phase). The vertical color scale from dark brown to white corresponds to an overall height of 15 nm.

Figure 5 Proposed model of rDGL distribution in homogenous galactolipid monolayer under gastric conditions

806 **Figure 1**

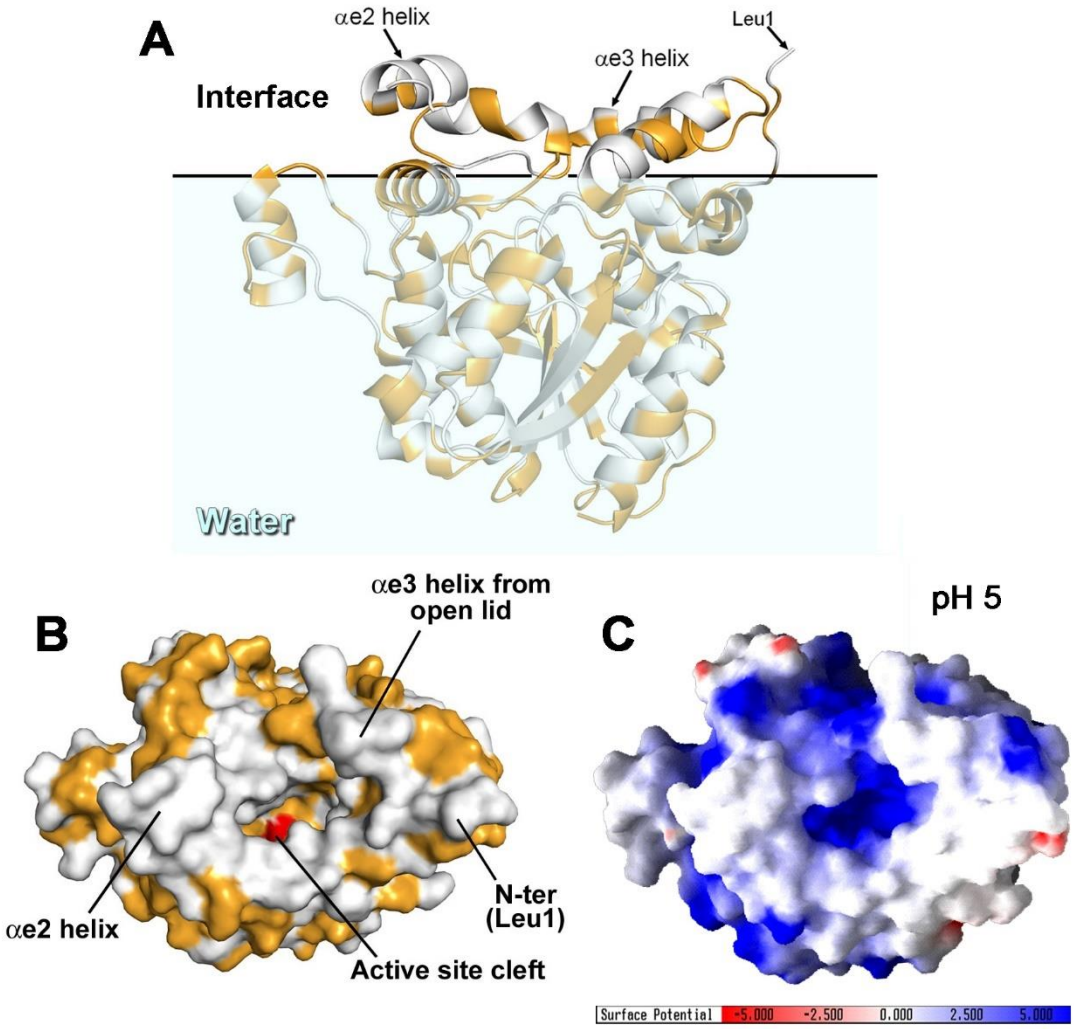

807

808

Figure 2

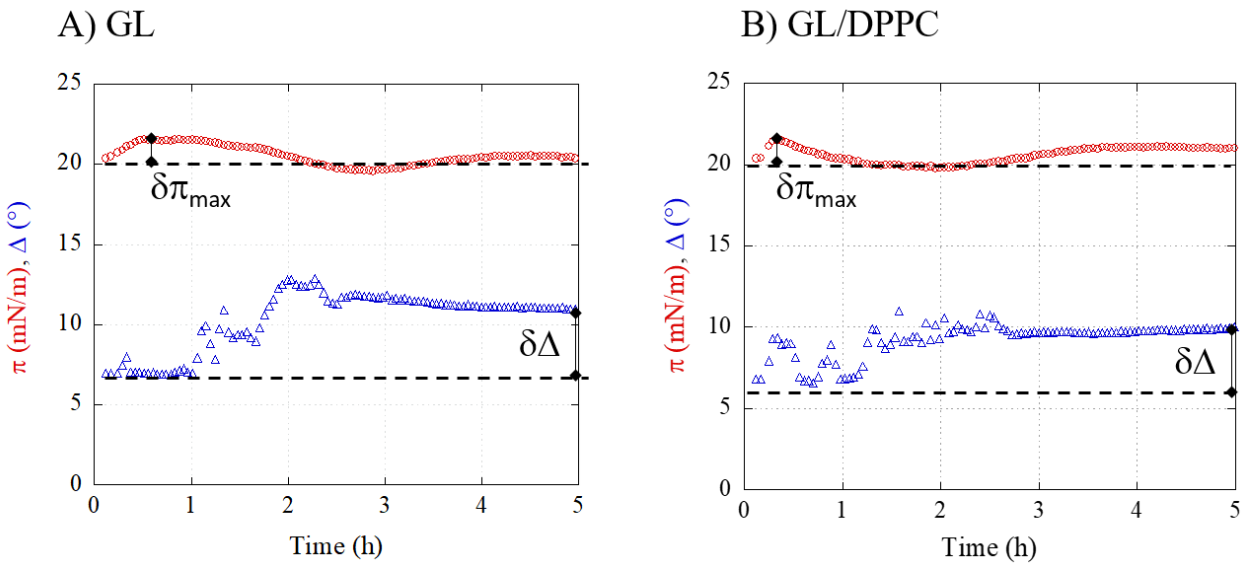

Figure 3

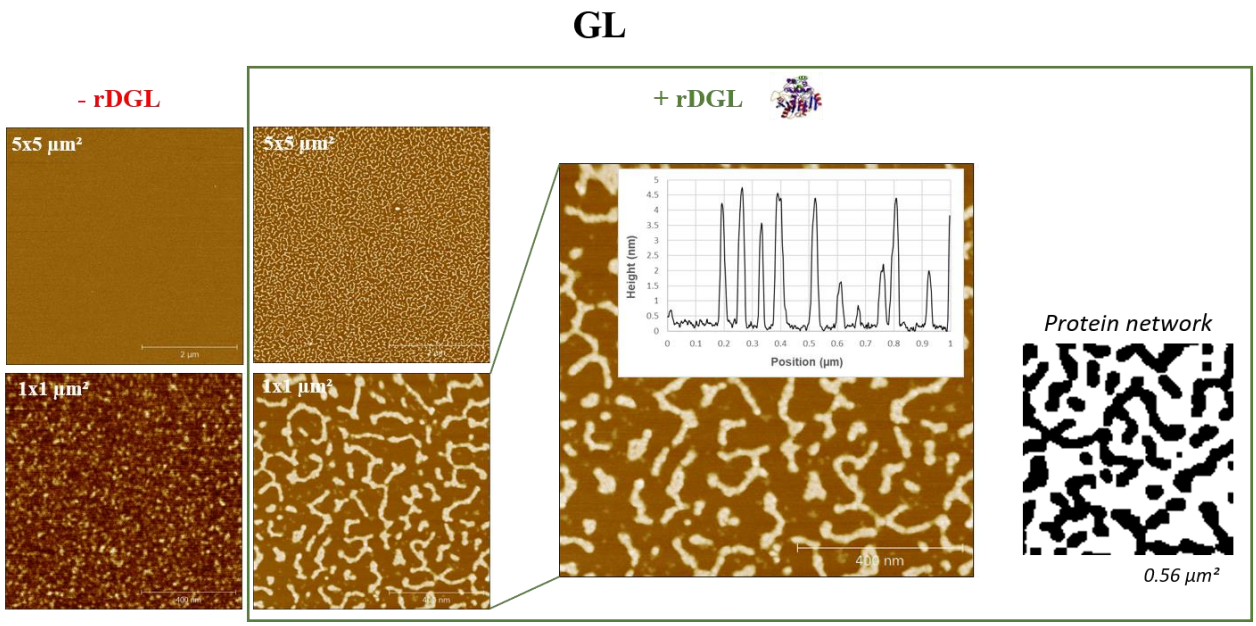

Figure 4

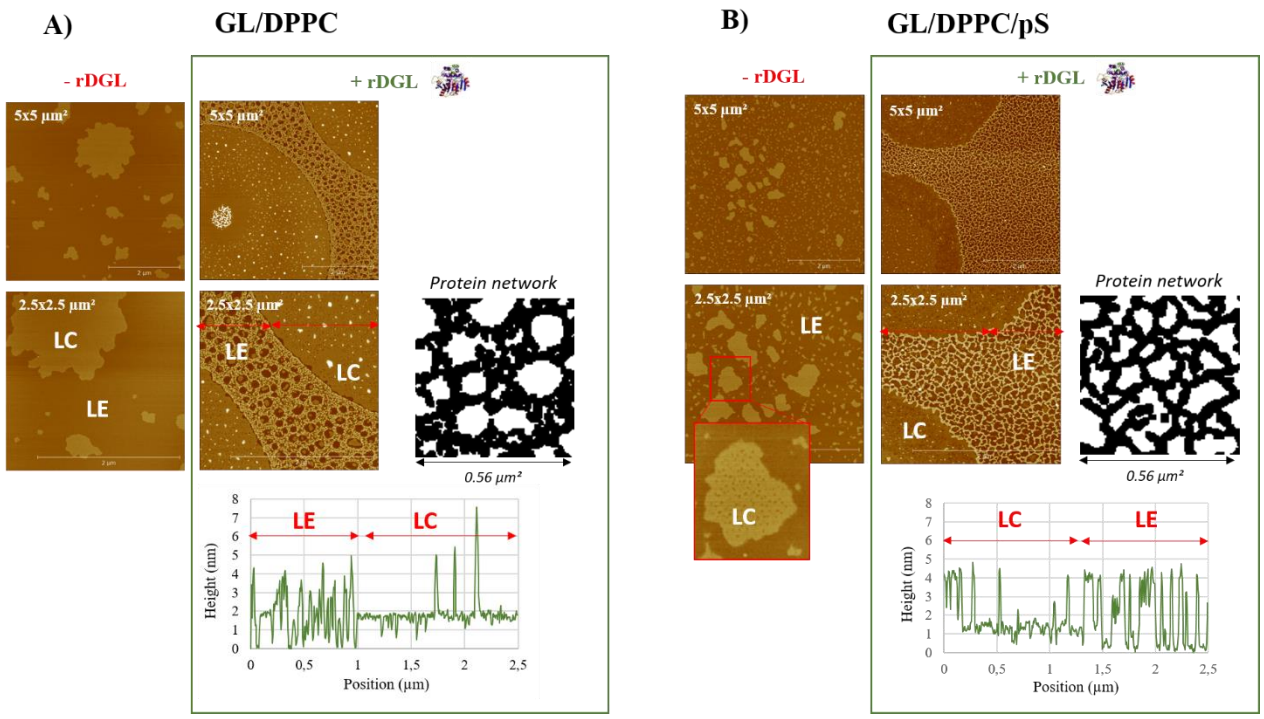

Figure 5

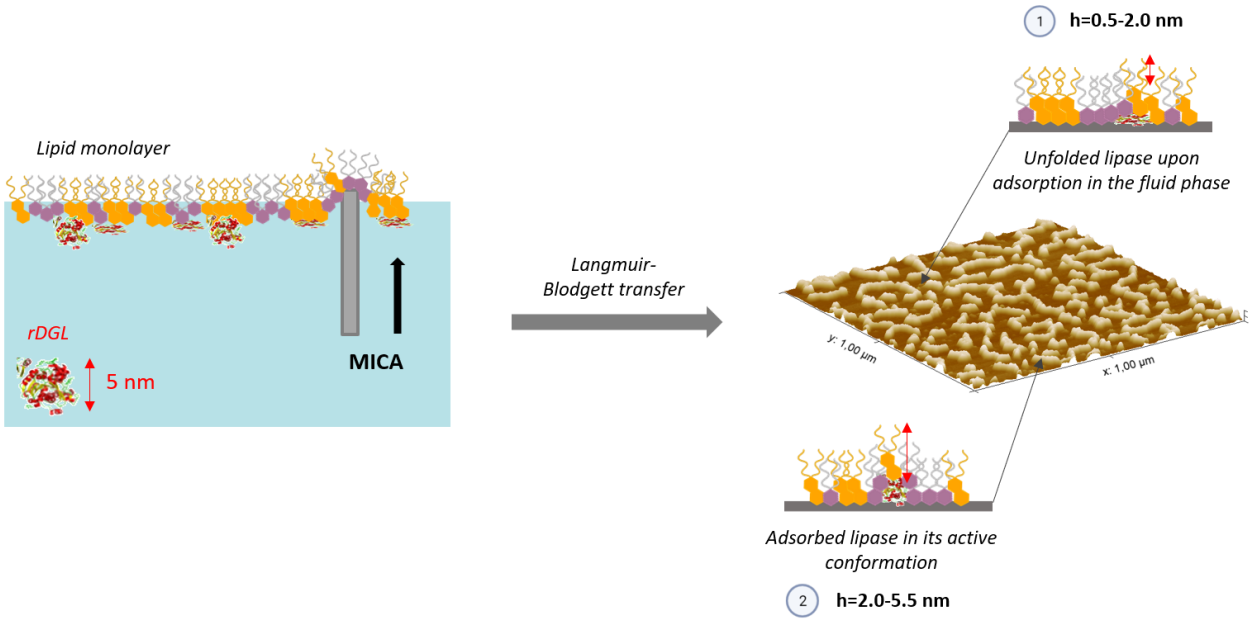

TABLES

Table 1 - Model system compositions

	Monolayer composition
(1) GL	MGDG/DGDG 60:40 mol/mol
(2) GL/DPPC	GL/DPPC 50:50 mol/mol
(3) GL/DPPC/pS	GL/DPPC/pS* 45:45:10 mol/mol/mol

**β-sitosterol, campesterol, brassicasterol 50:40:10 mol/mol/mol*

Table 2 - Summary of height levels identified in AFM images and related to rDGL interactions with model membranes. Height values are given in nm. The percentages given are the percentage of pixels covered by the indicated height range (-). Values obtained were based on the analysis of five plot profiles taken randomly in the AFM image.

Monolayer	Protein adsorption (nm)		
GL	h1 = 0.98 ± 0.4 (0.5 – 2) 17%	h2 = 2.0 ± 5.5 (2.0 – 5.5) 26%	-
$GL_{50}/DPPC_{50}$	h1 = 0.4 ± 0.1 (0.2 – 1.7) 32%	h2 = 2.6 ± 0.2 (2.3 – 4.8) 26%	h3 = 5.5 ± 0.7 (>5.5) 2%
$GL_{45}/DPPC_{45}/pS_{10}$	h1 = 1.2 ± 0.2 0.6 – 1.5 34%	h2 = 3.6 ± 0.6 (2.3 – 5.0) 24%	-